Magnetic and thermal stabilities of FeSiB eutectic amorphous alloys: Compositional effects

Shiqiang Yue [a, c, d], Hua Zhang [a, b, **], Rijin Cheng [a], Anding Wang [c, d, *], Yaqiang Dong [c], Aina He [c], Hongwei Ni [a, b], Chain-Tsuan Liu [d]

[a] The State Key Laboratory of Refractories and Metallurgy, Wuhan University of Science and Technology, No. 947 Hepingdadao Avenue, Qingshan District, Wuhan, 430081, China
[b] Key Laboratory for Ferrous Metallurgy and Resources Utilization of Ministry of Education, Wuhan University of Science and Technology, No. 947 Hepingdadao Avenue, Qingshan District, Wuhan, 430081, China
[c] Key Laboratory of Magnetic Materials and Devices, Ningbo Institute of Materials Technology and Engineering, Chinese Academy of Sciences, Ningbo, 315201, China
[d] Department of Materials Science and Engineering, City University of Hong Kong, Tat Chee Avenue, Kowloon Tong, Kowloon, Hong Kong, China

ARTICLE INFO

ABSTRACT

Magnetic and thermal stabilities of Fe-based amorphous alloys with high saturation flux density (B_s) are important for the application and understanding of the atomic interaction. $Fe_x(Si_3B_{13})_{(100-x)/16}$ ($x = 86$-71) eutectic amorphous alloys with superior manufacturability and Fe content limit were developed and the compositional effects were investigated. The alloys exhibit high B_s of 1.53−1.68 T, low coercivity of 2.2−4.3 A/m, and high permeability of $8.8−12.8 \times 10^3$. With the increase of Fe content, it is found that the B_s have an inflection point, the crystallization and Curie temperatures decrease drastically. The high Fe content alloys exhibit reduced thermal stabilities of magnetic properties, because the enhanced magnetic intercoupling effect is much lower than the weakened atomic bonding. For the alloys with $x = 71$−74, the decline rate of B_s is still lower than 10% at the extreme condition of 200 °C, while B_s of the alloy with $x = 84$ decreases more than 10% at 120 °C. The thermal stability of magnetic properties should be taken into consideration for the devices used in unique condition, especially for the high B_s amorphous alloys.

© 2018 Elsevier B.V. All rights reserved.

1. Introduction

Compared with conventional soft-magnetic crystalline materials, Fe-based amorphous alloys exhibit superior magnetic properties containing high saturation magnetic flux density (B_s), low coercivity (H_c), high permeability (μ_e) and much lower core loss [1]. These alloys have gradually taken critical roles in energy conservation and environmental protection [2], and been widely used in various electric devices [3,4]. Increasing efforts were hence devoted to develop new alloys with enhanced magnetic performance [5,6]

and unveil the property modulating mechanisms [7,8]. Hitherto, many alloy systems in large composition ranges have been reported to exhibit good performance at room temperature and their application potentials have been well publicized [9–12]. Nevertheless, the stabilities of magnetic properties, which are vital for the electric devices working at different temperature and frequency [13–17], were mentioned rarely. In addition, the thermal stability of the metastable amorphous alloys [18], directly correlates to the amorphous forming ability, annealing induced structural relaxation [19] and stress release [20], should be thoroughly evaluated. He et al. reported that the operating temperature has significant influence on the dynamic magnetic characteristics of commercial $Fe_{78}Si_9B_{13}$ alloy [21]. Mouhamad et al. found the core loss increased with the aging time and the lifetime of the $Fe_{82}Si_4B_{13}C_1$ was much shorter than the $Fe_{78}Si_9B_{13}$ alloy [22]. It is also well accepted that the Curie temperature (T_c) changes obviously with the compositions [23]. Recently, the limit of the Fe content of the amorphous alloys was broken and numerous high Fe content alloys were reported for high B_s, becoming a hot spot of this field [24,25]. These

* Corresponding author. Key Laboratory of Magnetic Materials and Devices, Ningbo Institute of Materials Technology and Engineering, Chinese Academy of Sciences, Ningbo, 315201, China.
** Corresponding author. The State Key Laboratory of Refractories and Metallurgy, Wuhan University of Science and Technology, No. 947 Hepingdadao Avenue, Qingshan District, Wuhan, China.
E-mail addresses: huazhang@wust.edu.cn (H. Zhang), anding@nimte.ac.cn (A. Wang).

one-sided emphases of the static magnetic properties are nowhere near enough. From the scientific aspects, the stabilities, reflecting the interaction of component elements, electric and cluster structures and etc. are important issues requiring more investigation [14,18].

In this study, $Fe_x(Si_3B_{13})_{(100-x)/16}$ ($x = 86, 84, 82, 80, 77, 74, 71$) eutectic amorphous alloys were developed by adjusting the composition and used for the investigation of compositional dependence of magnetic and thermal stabilities. The FeSiB eutectic amorphous alloys are typical model materials and expected to exhibit a low cost and a high manufacturability. We systematically studied the amorphous forming ability, crystallization and solidification behaviors, as well as the dependences of magnetic and thermal stabilities on the temperature and frequency. It is found that the increase of Fe content will lead to a peak of B_s and deteriorated stabilities of magnetic properties and T_c. Particular attention was paid to elucidate the mechanism of the temperature and frequency induced magnetic transition, and further to understand how the composition affects the stabilities.

2. Experiment procedures

Multicomponent alloy ingots with nominal compositions of $Fe_x(Si_3B_{13})_{(100-x)/16}$ ($x = 86, 84, 82, 80, 77, 74, 71$) were prepared by induction melting the mixtures of pure Fe (99.99 mass%), pure Si (99.99%), crystalline B (99.5 mass%) under a high-purity argon atmosphere. Ribbons with width of about 1 mm and thickness of about 30–38 μm were prepared by single copper roller melt-spinning method. The microstructures of ribbons were identified by X-ray diffraction (XRD) with Cu Kα radiation. Crystallization behaviors and thermal physical parameters containing Curie temperature (T_c) and crystallization temperature (T_X) of the amorphous alloy were analyzed by differential scanning calorimetry (DSC) at a heating rate of 0.67 °C/s. The liquid temperature of master alloys was also tested with (DSC) at a cooling rate of 0.067 °C/s to reduce the influence of undercooling. As the magnetic properties depend on the sample sizes, in the interest of clarification the intrinsic soft-magnetic properties of this amorphous alloy system, ribbon samples with similar size (width of about 1 mm and thickness of about 30 μm) were used for measurement. The intrinsic magnetic

properties including B_s and H_c were measured by a vibrating sample magnetometer (VSM) under an applied field of 800 kA/m and a DC B-H loop tracer, respectively. Effective permeability (μ_e) at frequency range of 1–100 kHz was measured with an impedance analyzer under a field of 1 A/m. Ribbon samples were annealed for 10 min by using an isothermal furnace under a low pressure of about 5×10^{-3} Pa in order to reduce the influence of inner stress on the above-mentioned properties for the investigation of the relaxation process. The microstructure of master alloys was observed by using a scanning electron microscope (SEM). The magnetic thermal (M-T) curves of the ribbons were also measured by VSM with a high temperature mode with a heating rate of 5 °C/min. Density (ρ) was measured by an Archimedean method.

3. Results and discussion

The melting and cooling behaviors obtained from DSC curves, measured with heating and cooling rates of 0.67 °C/s and 0.067 °C/s, are shown in Fig. 1a. The onset and off-set temperatures of the melting endothermic event shown in the heating section were designated by T_m and T_{lm}. The onset temperature of the solidification exothermic event shown in the cooling section is designated by T_{ls}. It is clear that all alloys exhibit single melting and crystallization peaks, which are typical characteristics of eutectic compositions [26]. It is interesting that all these alloys with large composition change are in the eutectic region and exhibit low T_m, T_{lm} and T_{ls}. The eutectic composition of the alloys was also proved by the eutectic solidification structure of the as-cast samples shown in Fig. 1d and e. The typical lamellar structures were found in alloys with Fe content of $x = 74$–80. For the alloys with high Fe content closed to the upper limit for fully amorphous phase formation of $x = 86$ and lower limit of $x = 71$ for ductile ribbon formation, the structure changed into ball-like and rod-like regular shapes. It has been proved that eutectic alloys are characterized with thermo-dynamic and kinetic advantages, including low crystallization driving energy, large undercooling ability, sluggish diffusion rate and competing precipitation effects, for high amorphous forming ability [27]. In addition, since eutectic alloy liquids always have good fluidity, these alloys should exhibit excellent casting property. The good amorphous forming ability and manufacturability of the
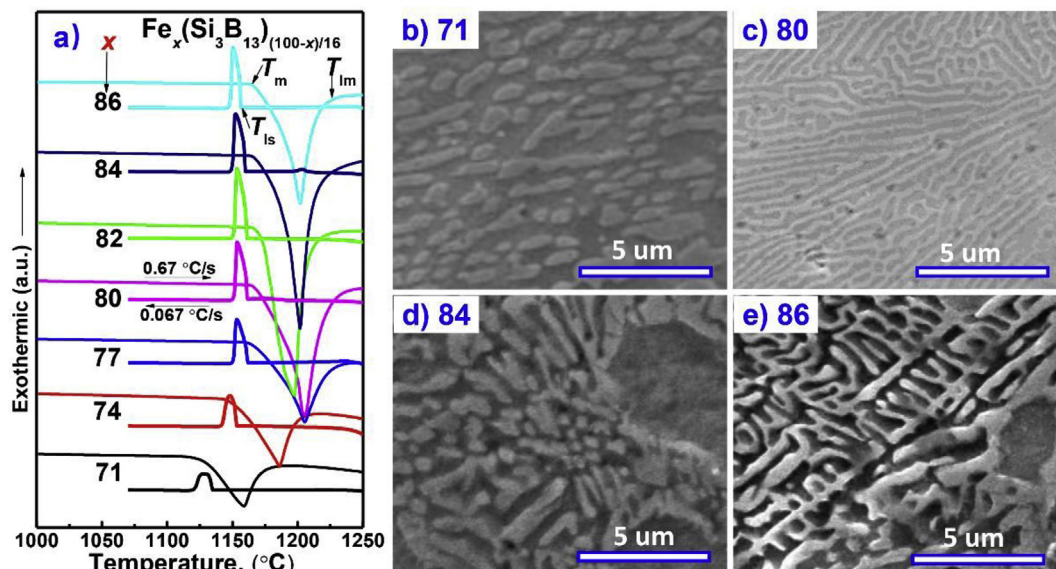

Fig. 1. a) DSC curves of $Fe_x(Si_3B_{13})_{(100-x)/16}$ ($x = 86$-71) master alloys showing the melting and solidification behaviors; b-e) The SEM images of microstructure of representative $Fe_x(Si_3B_{13})_{(100-x)/16}$ ($x = 86,84, 80, 71$) master alloys.
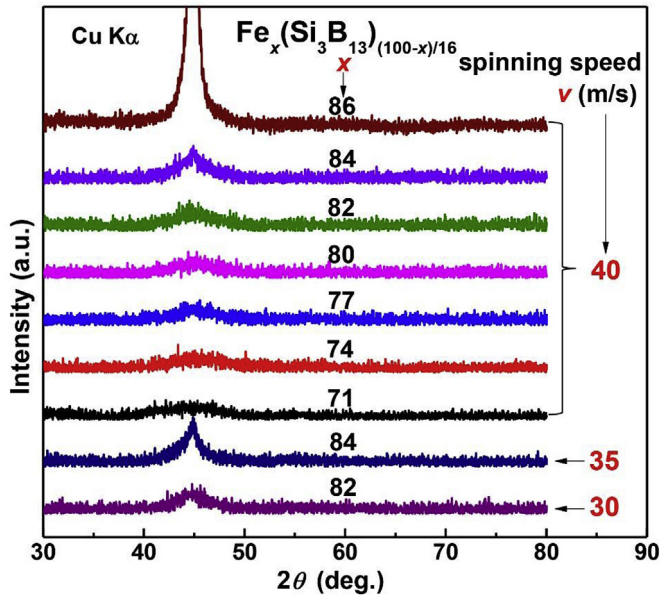
Fig. 2. XRD patterns of the $Fe_x(Si_3B_{13})_{(100-x)/16}$ ($x = 86$-71) alloy ribbons with critical spinning speed (v) and used for magnetic measurement.

$Fe_x(Si_3B_{13})_{(100-x)/16}$ ($x = 86, 84, 82, 80$) alloys have been verified in our recent industrialization experiments.

By adjusting the spinning speed (v) for ribbon production, the amorphous forming ability of the $Fe_x(Si_3B_{13})_{(100-x)/16}$ ($x = 86, 84, 82, 80, 77, 74, 71$) alloys was evaluated according to the critical v and thickness. As shown in Fig. 2, the critical v for the alloys with $x = 82$ and 84 are 30 m/s and 40 m/s. It is hard to prepared fully amorphous ribbon samples even using a high v of 50 m/s, indicating the Fe content of 86 at. % has exceed the limit of this alloy system. It is easy to prepare amorphous ribbons with high ductility and surface quality for the alloys with $x = 82$-74, by using the industry acceptable v of 20−30 m/s [28]. All ribbons made with v of 40 m/s for subsequent magnetic and thermal measurement exhibit amorphous microstructure shown in Fig. 2 and good surface quality.

Fig. 3 shows the DSC curve of the as-spun $Fe_x(Si_3B_{13})_{(100-x)/16}$ ($x = 84, 82, 80, 77, 74, 71$) ribbons. It is clear that the T_c and T_x

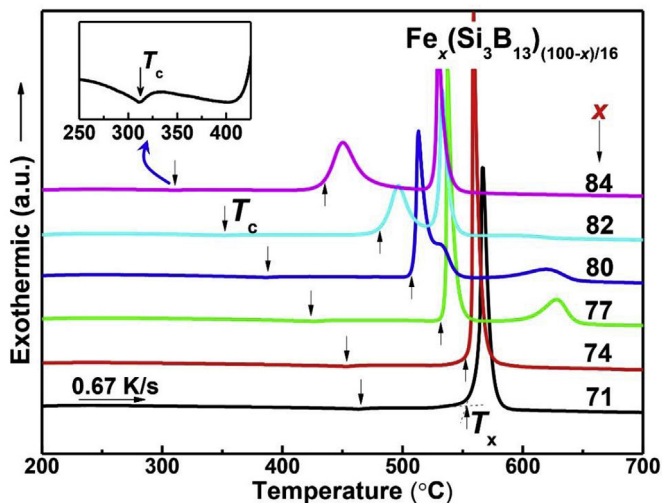decrease substantially with the increase of Fe content, from 463 °C to 310 °C and from 564 °C to 434 °C, respectively. The temperature interval between Curie transition and crystallization (T_X -T_c) increases and keeps high values more than 100 °C. In order to attain superior soft-magnetic properties, annealing for free volume annihilation, microstructure homogenization without crystallization and release of inner stress, should be performed between the T_c and T_X. The large T_X-T_c should be an important indicator for excellent soft-magnetic properties. In addition, it has been reported that the low T_c is good for improving the ductility of the annealed ribbons [29]. On the other hand, the low T_c and T_X mean the low thermal stability of magnetic transition, structural relaxation and crystallization [30], which will be investigated in detailed. The increase of Fe content also leads to change of crystallization behaviors. For the alloys with x = 71 and 74, competing crystallization occurs in one peak. The crystallization peak splits into two distinct peaks for the alloys with higher Fe content.

Isothermal annealing was performed at the temperature ranged from 200 °C to T_x-50 °C and static magnetic properties were tested, to explore the optimal properties and correlated processes. Fig. 4 shows the annealing temperature (T_A) dependence of H_c and μ_e at 1 kHz. All alloys show similar change trends: H_c decreases gradually with the increase of the T_A and reaches the lowest value of 2.2−4.3 A/m, μ_e increases first to the peak values of 10.2−12.8 × 10³ and decreases then. The optimal magnetic properties of all alloys are excellent, especially for the alloys with $x = 82$-74. It should be noting that the optimal T_A of the high Fe content alloy with x = 84 is only 320 °C, which is about 160 °C lower than the alloy with x = 71. The low T_A annealing at 200 °C for 10 min can improve the soft-magnetic properties. Since the annealing induced structure relaxation is co-affected by T_A and annealing time (t), the lifetime of the ribbons working in extreme heating conditions (120 °C of international standard) should decrease drastically with the increase of Fe content [22].

Since the amorphous alloy cores are used in diversified devices with difference frequency (f), the μ_e stability is a very important parameter. Fig. 5 shows the dependence of μ_e on f of the optimally annealed ribbon samples. At f lower than 10 kHz, all alloys exhibit superior μ_e higher than 6×10^3. All curves decrease with the increase of f from low f to the cut-off f of about 20 kHz. It is interesting

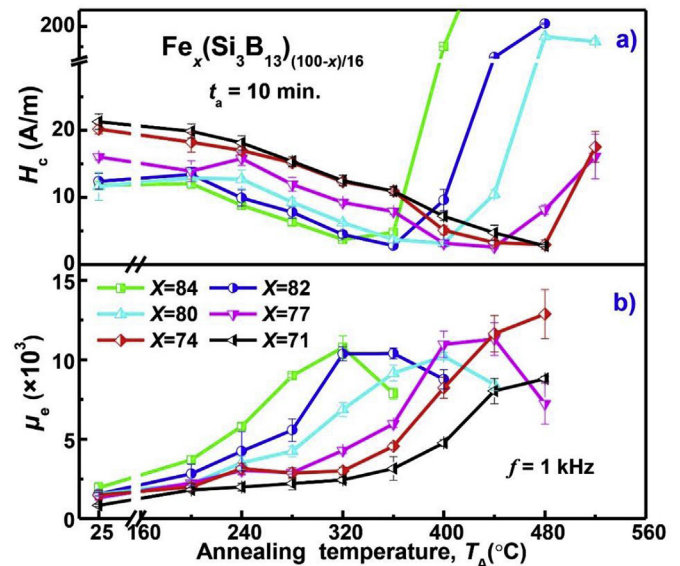**Fig. 3.** DSC curves of the $Fe_x(Si_3B_{13})_{(100-x)/16}$ ($x = 84$-71) amorphous alloys showing the crystallization behavior.

Fig. 4. Annealing temperature (T_A) dependence of H_c and μ_e at 1 k Hz for $Fe_x(Si_3B_{13})_{(100-x)/16}$ ($x = 84$-71) amorphous alloys annealed for 10 min.
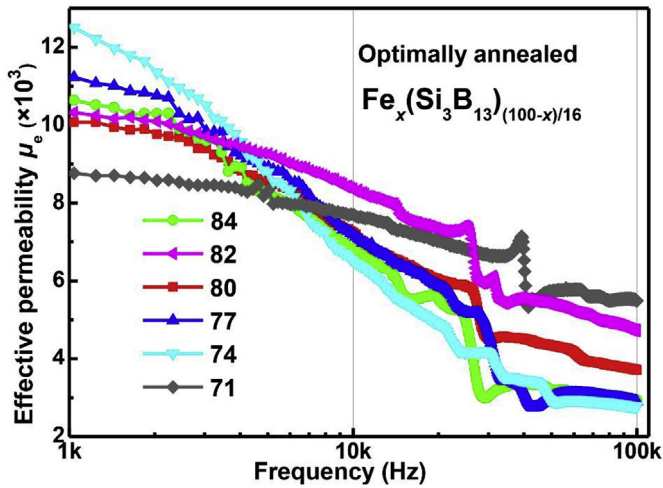
Fig. 5. Effective permeability (μ_e) as a function of applied field frequency (f) for the Fe$_x$(Si$_3$B$_{13}$)$_{(100-x)/16}$ ($x=84-71$) amorphous alloy ribbons annealed for 10 min at optimum temperature.

Fig. 7. a) Fe content dependences of T_c attained from the M-T and DSC curves of the Fe$_x$(Si$_3$B$_{13}$)$_{(100-x)/16}$ ($x=84-71$) amorphous alloys; b) The M_s, ρ and B_s as functions of Fe content.

that the μ_e of the alloys with higher μ_e at 1 kHz declines faster. The alloys with $x=82$ shows better f stability of μ_e. As is known that the μ_e and f stability can also be readily modulated by magnetic and stress annealing [31], the Fe$_x$(Si$_3$B$_{13}$)$_{(100-x)/16}$ ($x=84-71$) amorphous alloys are expected to exhibit more attractive μ_e and f stability than the conventional electric steels.

Fig. 6a shows the saturated magnetic moment (M_s) vs temperature (M-T) curve of the optimally annealed Fe$_x$(Si$_3$B$_{13}$)$_{(100-x)/16}$ ($x=84-71$) amorphous alloy ribbons. Consistent with the change tendency of T_c obtained from the DSC curves, the T_c on M-T curves increase gradually with the increase of Fe content. It is clear that the M_s of all alloys decreases drastically at the temperature of 150–200 °C below the T_c and the low Fe content alloys exhibit the best thermal stability of M_s. Even at low temperature range of room temperature to 120 °C, the high Fe content alloys suffer obvious decrease of M_s, which should be carefully handled for the application in transformers and motors in an over load condition. Since
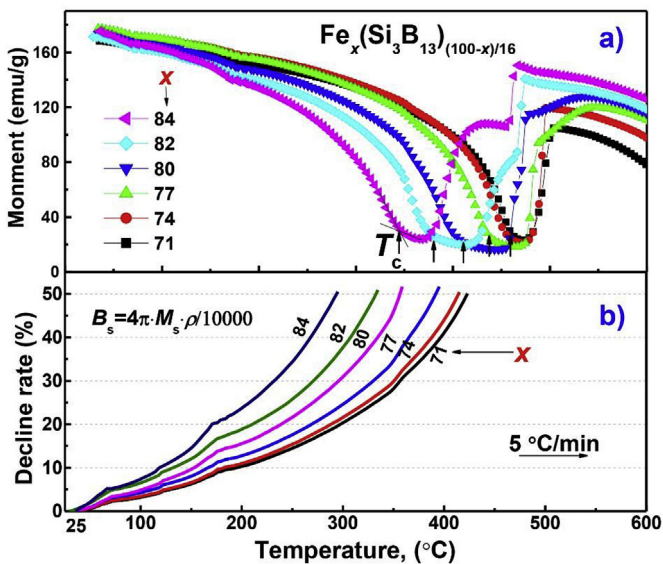

Fig. 6. a) Magnetic moment vs temperature (M-T) curve of the optimally annealed Fe$_x$(Si$_3$B$_{13}$)$_{(100-x)/16}$ ($x=84-71$) amorphous alloy ribbons, b) Decline rate of the B_s as a function of temperature, compared with the value measured at room temperature.
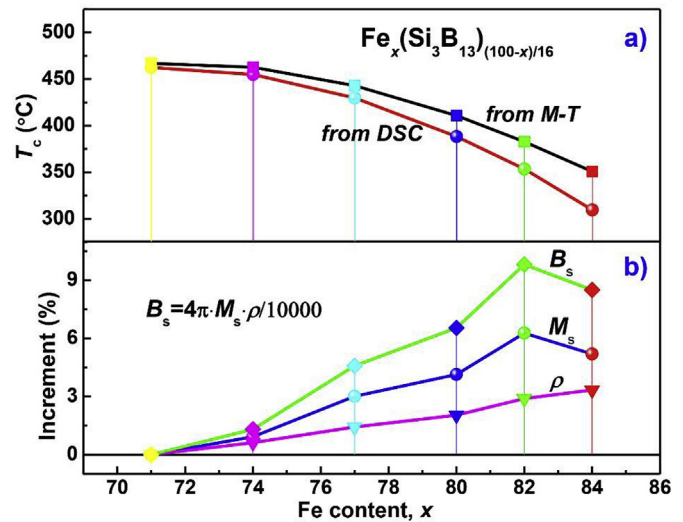
the density (ρ) changes little with the temperature, the B_s is proportionate to the M_s. As shown in Fig. 6b, compared with the B_s measured at room temperature, the decline rate of B_s for the alloy with $x=84$ is higher than 10% at 120 °C. For the alloys with $x=71$ and 74, the decline rate of B_s is still lower than 10% at the extreme condition of 200 °C. Therefore, the thermal stability of B_s should be take into consideration for the devices used in unique condition.

According to the former results, we can draw an important point about the T_c, which correlates to the thermal stability of B_s and is a key parameter for determining the annealing temperature. However, the values of the obtained from the DSC and M-T curves are quite different, although exhibit the same variation trend. As shown in Fig. 7a, The T_c value obtained from the DSC curves is lower than the M-T curves. This is understandable because the small valley in DSC curve reflects the most drastic transition temperature, while the T_c point in a M-T curve means the end of the transition. Here, we want to note that the difference between the T_c values obtained from two measurement increases greatly with the increase of Fe content, indicating the decrease of the thermal stability also.

There is always a misunderstanding that the advantage of high B_s will be discounted by the increase of ρ of high content Fe-based alloy. Fig. 7b shows the dependences of M_s, ρ and B_s of Fe$_x$(Si$_3$B$_{13}$)$_{(100-x)/16}$ ($x=84-71$) amorphous alloys on Fe content. Compared with the value of the alloy with $x=71$, the ρ increases gradually. The M_s increases first at reaches a peak value of 177.3 emu/g for the alloy with $x=82$. Since the B_s is a product ρ and M_s, the B_s increase with a higher increment. The ρ and M_s, the B_s of the alloy with $x=82$ are 2.9%, 6.3% and 9.8% higher than that of the lowest Fe content alloy. In addition, there are peaks for the M_s, and B_s, consistent with the former reports [32]. It is hence illustrated that the advantage of B_s will be amplified, for the high Fe content alloys, except the one exceeds the peak value.

Table 1 gathers the thermal parameters and optimal magnetic properties of Fe$_x$(Si$_3$B$_{13}$)$_{(100-x)/16}$ ($x=84-71$) amorphous alloys. The FeSiB system alloys exhibit controllable and attractive magnetic properties, which can be adjusted according to the application requirement. The T_{lm} and T_{ls} changes slightly, indicating a similar ribbon production process and good manufacturability. The B_s, T_c and T_x changes gradually, with the increase of Fe content. According to the static magnetic properties, the Fe$_{82}$(Si$_3$B$_{13}$)$_{18/16}$ alloy is the

Table 1
Thermal parameters and optimal magnetic properties of $Fe_x(Si_3B_{13})_{(100-x)/16}$ (x = 84-71) amorphous alloys.

Constitution	Thermal properties					Magnetic properties		
	T_c(°C)	T_{x1}(°C)	T_m(°C)	T_{lm}(°C)	T_{ls}(°C)	B_s(T)	H_c(A/m)	$\mu_e(10^3)$
$Fe_{84}Si_3B_{13}$	310	434	1186	1210	1159	1.66	4.3	10.8
$Fe_{82}(Si_3B_{13})_{18/16}$	353	483	1173	1205	1161	1.68	2.2	10.4
$Fe_{80}(Si_3B_{13})_{20/16}$	388	510	1192	1218	1161	1.63	2.6	10.2
$Fe_{77}(Si_3B_{13})_{23/16}$	430	536	1185	1222	1162	1.60	2.3	11.3
$Fe_{74}(Si_3B_{13})_{26/16}$	455	558	1155	1199	1153	1.55	2.2	12.8
$Fe_{71}(Si_3B_{13})_{29/16}$	463	564	1129	1172	1135	1.53	2.2	8.8

best. The $Fe_{84}Si_3B_{13}$ alloy exhibits deteriorated magnetic properties, poor amorphous formability, and lowest thermal stability.

The above results show that the magnetic and thermal stabilities of the $Fe_x(Si_3B_{13})_{(100-x)/16}$ (x = 84-71) alloys vary significantly with the Fe content. Subsequently, the mechanism of the microstructure changes and its influence on the stabilities will be discussed in details. First, we explore the reasons for the eutectic composition in large composition range and high Fe content limit based on high amorphous forming ability. According to the binary phase diagrams of Fe-B and Fe-Si, the eutectic point of Fe-B is17 at. % and the Fe and Si are mutually soluble in large range. The precipitation phases of the $Fe_x(Si_3B_{13})_{(100-x)/16}$ (x = 84-71) alloys are α-Fe(Si) solution and Fe_2B compound. The variable content of the Si in α-Fe(Si) solution widens the eutectic composition range effectively [9]. In addition, Si exhibits larger atom size and negative mixing enthalpy with Fe than B, leading to an enhanced amorphous forming ability and higher Fe content limit [18]. Compared with the commercial $Fe_{78-80}Si_9b_{11-13}$ alloys, the decrease of Si content of this alloy system are also important for the breakthrough of Fe content limit and approaching the eutectic composition range. Second, the decrease of magnetic and thermal stability with increase of Fe content will be discussed. Since the Si and B are small atom occupying the interstitial of Fe and exhibit attractive effects with Fe atoms, the addition will lead to a tightened and close packing structure [33]. The interaction between Fe and Si/B atoms will increase, resulting a more stable structure. As shown in Fig. 8, the primary crystallization phase of low Fe content alloy is metastable Fe_3B which will resolve to Fe_2B and α-Fe(Si). The amorphous structure of the low Fe content alloy will be more stable. For the high Fe content alloys, the primary phase is α-Fe(Si) which will precipitate more earlier in the Fe-based alloys at low temperature.

Furthermore, the magnetic intercoupling interaction effect of Fe atoms is much poorer than atomic bonding, which is also the reason why high Fe content alloy exhibit higher a B_s and a poorer stability of magnetic properties.

4. Conclusion

$Fe_x(Si_3B_{13})_{(100-x)/16}$ (x = 86, 84, 82, 80, 77, 74, 71) eutectic amorphous alloys were developed by adjusting the composition. The compositional dependence of magnetic and thermal stabilities, amorphous forming ability, as well as crystallization and solidification behaviors were investigated systematically.

1) The FeSiB eutectic amorphous alloys exhibit attractive magnetic properties, containing high B_s of 1.53−1.68 T, low H_c of 2.2−4.3 A/m, and high μ_e of 8.8−12.8 × 10^3.
2) The crystallization and Curie temperatures decrease drastically with the increase of Fe content, from 564 °C to 434 °C and 463 °C to 310 °C. The liquidus temperature changes slightly in the large composition range.
3) The high Fe content alloys exhibit reduced thermal stabilities of magnetic properties. Compared with the B_s measured at room temperature, the decline rate of B_s for the alloy with x = 84 is higher than 10% at 120 °C. For the alloys with x = 71 and 74, the decline rate of M_s is still lower than 10% at the extreme condition of 200 °C. The reduced stability can be attributed to the much poorer magnetic intercoupling effect than the atomic bonding.
4) The FeSiB eutectic amorphous alloys are typical model materials for basic study of compositional effects and expected to have attractive application prospects. The thermal stability of magnetic properties should be taken into consideration for the devices used in unique condition, especially for the high B_s amorphous alloys.

Acknowledgements

References

[1] M.E. McHenry, M.A. Willard, D.E. Laughlin, Amorphous and nanocrystalline materials for applications as soft magnets, Prog. Mater. Sci. 44 (1999) 291−433.
[2] O. Gutfleisch, M.A. Willard, E. Brück, C.H. Chen, S.G. Sankar, J.P. Liu, Magnetic materials and devices for the 21st century: stronger, lighter, and more energy efficient, Adv. Mater. 23 (2011) 821−842.
[3] Y.H. Chang, C.H. Hsu, H.W. Lin, C.P. Tseng, Reducing audible noise for distribution transformer with HB1 amorphous core, J. Appl. Phys. 109 (2011) 3.
[4] Y. Zhang, J.L. Liu, Physical suppression effects of the reversed magnetic coupling on the saturation inductance of saturable pulse transformer, Appl. Phys. Lett. 102 (2013) 5.
[5] R. Hasegawa, D. Azuma, Impacts of amorphous metal-based transformers on energy efficiency and environment, J. Magn. Magn. Mater. 320 (2008)
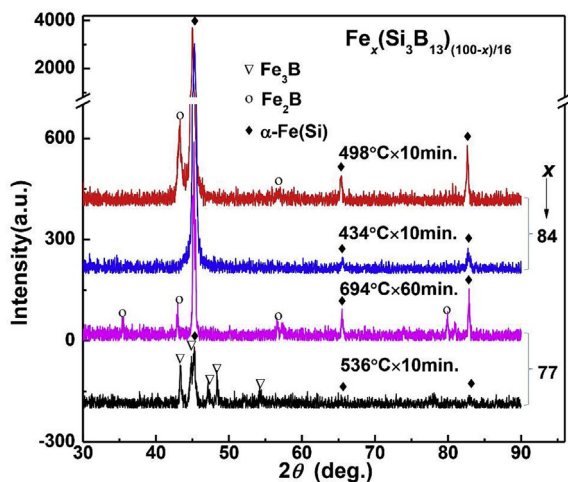
Fig. 8. XRD patterns of the representative alloy ribbons annealed for precipitation phase identification.

2451–2456.

[6] A.D. Wang, C.L. Zhao, H. Men, A.N. He, C.T. Chang, X.M. Wang, R.W. Li, Fe-based amorphous alloys for wide ribbon production with high B-s and outstanding amorphous forming ability, J. Alloys Compd. 630 (2015) 209–213.

[7] B. Huang, Q.F. He, A.D. Wang, C.L. Zhao, Q. Wang, Y. Yang, C.T. Liu, Tunable elastic heterogeneity caused by deformation-induced magnetization in flexible metallic glass, Scripta Mater. 130 (2017) 7–11.

[8] B. Sarac, Y.P. Ivanov, A. Chuvilin, T. Schöberl, M. Stoica, Z. Zhang, J. Eckert, Origin of large plasticity and multiscale effects in iron-based metallic glasses, Nat. Commun. 9 (2018) 1333.

[9] A.D. Wang, C.L. Zhao, A.N. He, H. Men, C.T. Chang, X.M. Wang, Composition design of high B-s Fe-based amorphous alloys with good amorphous-forming ability, J. Alloys Compd. 656 (2016) 729–734.

[10] T. Hibino, T. Bitoh, Ternary Fe-B-C and quaternary Fe-B-C-Si amorphous alloys with glass transition and high magnetization, J. Alloys Compd. 707 (2017) 82–86.

[11] F. Wang, A. Inoue, Y. Han, F.L. Kong, S.L. Zhu, E. Shalaan, F. Al-Marzouki, A. Obaid, Excellent soft magnetic Fe-Co-B-based amorphous alloys with extremely high saturation magnetization above 1.85 T and low coercivity below 3 A/m, J. Alloys Compd. 711 (2017) 132–142.

[12] J.F. Wang, W.B. Cao, L.G. Wang, S.J. Zhu, S.K. Guan, L. Huang, R. Li, T. Zhang, Fe-Al-P-C-B bulk metallic glass with good mechanical and soft magnetic properties, J. Alloys Compd. 637 (2015) 5–9.

[13] A.N. He, S.Q. Yue, A.D. Wang, C.T. Chang, X.M. Wang, Dynamic magnetic characteristics and relaxation of Fe73.5Cu1Nb3Si15.5B7 nanocrystalline alloy under operating temperature and magnetizing frequency, J. Magn. Magn. Mater. 443 (2017) 261–266.

[14] P. Vojtanik, Magnetic relaxations in amorphous soft magnetic alloys, J. Magn. Magn. Mater. 304 (2006) 159–163.

[15] K.G. Efthimiadis, G. Stergioudis, S.C. Chadjivasiliou, I.A. Tsoukalas, On magnetic properties and thermal stability of Fe(M)Si-B (M = V, Ni, Cu, Nb, Mo, Pd, Ag) amorphous alloys, Cryst. Res. Technol. 37 (2002) 827–833.

[16] P. Haussler, D. Moorhead, R. Hauert, H. Poppa, E. Kay, Influence of indirect magnetic interaction on the stability of amorphous-alloys, J. Non-Cryst. Solids 117 (1990) 293–296.

[17] T. Reininger, M. Vazquez, H. Kronmuller, Temperature-dependence of the magnetic-properties of a co-rich amorphous alloy after field, stress, and stress-field annealing, Phys. Status Solidi A Appl. Res. 132 (1992) 477–486.

[18] A. Inoue, Stabilization of metallic supercooled liquid and bulk amorphous alloys, Acta Mater. 48 (2000) 279–306.

[19] M. Nabialek, Soft magnetic and microstructural investigation in Fe-based amorphous alloy, J. Alloys Compd. 642 (2015) 98–103.

[20] T. Bitoh, A. Makino, A. Inoue, Origin of low coercivity of (Fe0.75B0.15Si0.10)(100-x)Nb-x (x=1-4) glassy alloys, J. Appl. Phys. 99 (2006), 08F102.

[21] A. He, A. Wang, S. Yue, C. Zhao, C. Chang, H. Men, X. Wang, R.-W. Li, Dynamic magnetic characteristics of Fe78Si13B9 amorphous alloy subjected to operating temperature, J. Magn. Magn. Mater. 408 (2016) 159–163.

[22] M. Mouhamad, C. Elleau, F. Mazaleyrat, C. Guillaume, B. Jarry, Physicochemical and accelerated aging tests of metglas 2605SA1 and metglas 2605HB1 amorphous ribbons for power applications, IEEE Trans. Magn. 47 (2011) 3192–3195.

[23] K. Narita, H. Fukunaga, J. Yamasaki, Effects of metalloid content on curie-temperature and magnetic-moment of amorphous Fe-Si-B alloys, Jpn. J. Appl. Phys. 16 (1977) 2063–2064.

[24] P.B. Chen, A.D. Wang, C.L. Zhao, A.N. He, G. Wang, C.T. Chang, X.M. Wang, C.T. Liu, Development of soft magnetic amorphous alloys with distinctly high Fe content, Sci. China Phys. Mech. 60 (2017) 6.

[25] J.F. Li, X. Liu, S.F. Zhao, H.Y. Ding, K.F. Yao, Fe-based bulk amorphous alloys with iron contents as high as 82 at%, J. Magn. Magn. Mater. 386 (2015) 107–110.

[26] L.L. Shi, J. Xu, E. Ma, Alloy compositions of metallic glasses and eutectics from an idealized structural model, Acta Mater. 56 (2008) 3613–3621.

[27] A.R. Yavari, Solving the puzzle of eutectic compositions with 'miracle glasses', Nat. Mater. 4 (2005) 2–3.

[28] J. Pang, A.D. Wang, S.Q. Yue, F.Y. Kong, K.Q. Qiu, C.T. Chang, X.M. Wang, C.T. Liu, Fluxing purification and its effect on magnetic properties of high-B-s FeBPSiC amorphous alloy, J. Magn. Magn. Mater. 433 (2017) 35–41.

[29] X. Liang, A. He, A. Wang, J. Pang, C. Wang, C. Chang, K. Qiu, X. Wang, C.-T. Liu, Fe content dependence of magnetic properties and bending ductility of FeSiBPC amorphous alloy ribbons, J. Alloys Compd. 694 (2017) 1260–1264.

[30] H.B. Yu, W.H. Wang, K. Samwer, The beta relaxation in metallic glasses: an overview, Mater. Today 16 (2013) 183–191.

[31] C. Miguel, A.P. Zhukov, J.J. del Val, A.R. de Arellano, J. Gonzalez, Effect of stress and/or field annealing on the magnetic behavior of the (Co77Si13.5B9.5)(90) Fe7Nb3 amorphous alloy, J. Appl. Phys. 97 (2005) 8.

[32] T. Masumoto, Amorphous magnetic-alloys, Sci. Rep. Res. Inst. Tohoku Univ. A 29 (1981) 265–275.

[33] D.B. Miracle, W.S. Sanders, O.N. Senkov, The influence of efficient atomic packing on the constitution of metallic glasses, Philos. Mag. 83 (2003) 2409–2428.